DOI: 10.1002/zaac.201300208

Synthesis, Crystal Structure, and Properties of the First Organomercury Dimer Derived from PMP

Rui-Bo Xu,*[a,b] Wei-Xing Ma,[a] Jia-Bin Qi,[a] Yi-Qiu Qin,[a] Jia-Wei Zhang,[a] Shu-Ping Yang,[a] and Xing-You Xu[c]

Keywords: 1-Phenyl-3-methyl-2-pyrazolin-5-one; Organomercury chloride; Crystal structure; Thermal stability; Bioactivity

Abstract. The organomercury dimer $[Hg_2(PMP)Cl_2]_2$·DMF (**1**) (PMP = 1-phenyl-3-methyl-2-pyrazolin-5-one) was prepared by the reaction of mercury chloride with PMP and characterized by elemental analysis, IR spectroscopy, TG, and single-crystal X-ray diffraction analysis. The title compound crystallizes in the triclinic space group $P\bar{1}$, with a = 7.4298(6), b = 9.0313(8), c = 12.4145(13) Å, V = 760.50(12) Å^3, Z = 1. Each mercury(II) atom is tricoordinated to one chlorine atom, one carbon atom of the pyrazole ring from one PMP, and one oxygen atom from another PMP. The coordination arrangement around the mercury atom is T-shaped. This is the first structural report on an organomercury derivative of PMP. The distance between the two Hg^{II} ions is 3.2735(8) Å, which indicates the presence of weak Hg···Hg interactions. Meanwhile, **1** can be connected by intermolecular C–H···Cl hydrogen bonding and weak Hg···O/Cl/N interactions to form a three dimensional network. The thermal stability and antibacterial activity of **1** were studied. The binding of **1** with calf thymus DNA was investigated by absorption spectroscopy and viscometry.

1 Introduction

Mercury is well-known as a toxic element,[1] which has received increasingly scientific attention.[1–3] Mercury metal, mercury salts, and organomercury compounds are ubiquitous and can be persistent environmental toxins. However, organomercury compounds have become one of the most investigated organometallic reagents for the introduction of a variety of functional groups in predefined organic skeletons,[3,4] synthesis of other organometallic compounds by transmetalation,[5,6] formation of various functional coordination complex, and removement of mercury ions from aqueous solution by coordination with suitable ligands.[7–9]

Pyrazolone derivatives, characterized as a five-membered ring lactam, are important frameworks, which exhibit variety of applications such as pharmaceutical candidates, biologically important structural components.[10,11] Edaravone (1-phenyl-3-methyl-2-pyrazolin-5-one; PMP) is an important intermediate for dyes and pharmaceuticals, and had been used to treat the acute stage cerebral infarction.[12–14] Just like other ligands containing N and O donors, PMP can display several different coordination modes[15–19]. For many years, we have been interested in the construction of metal complexes derived from PMP, and synthesized some PMP complexes such as $[Zn(PMP)_2Cl]_n$,[15] $[Cd(PMP)_2]_n$,[16] and $[Cd_2(PMP)_2Cl_4]_n$[17]. As a continuation of our work, we have prepared another novel organomercury compound, $[Hg_2(PMP)Cl_2]_2$·DMF (**1**). In **1**, each Hg^{II} is coordinated to O, C, and Cl atoms, adopting a T-shaped arrangement. Compound **1** contains weak mercurophilic interactions [Hg···Hg distance of 3.2735(1) Å].[5,20,21] It is well known that the mercury ion can easily attack alkanes to form new metal–C(sp^3) bonds or aromatic compounds to form metal–C(sp^2) bonds.[3,20,22] Moreover, regioselective mono-metalation or di-metalation usually takes place at C-2, C-4, C-6, or C-4,6 of the benzene ring.[3,19,20,23] Nevertheless, the Hg^{II} ion of **1** is covalently bonded to the C2 of the pyrazolone ring and not to the benzene ring. Regioselective metalation of pyrazolone ring has not yet been reported. Hence this is the first case of mercuric-PMP. Herein, we report the synthesis, crystal structure, thermal stability, antibacterial activity, and DNA-bonding property of the novel organomercury dimer **1**.

* Dr. R.-B. Xu
Fax: +86-581-85895085
E-Mail: xuruibo9125@163.com
[a] School of Chemical Engineering
Huaihai Institute of Technology
Lianyungang 222005, P.R. China
[b] State Key Laboratory of Analytical Chemistry for Life Science
School of Chemistry and Chemical Engineering
Nanjing University
Nanjing 210093, P.R. China
[c] Huaiyin Institute of Technology
Huaian 223003, P.R. China

2 Experimental Section

2.1 Synthesis of $[Hg_2(PMP)Cl_2]_2$·DMF (1)

A solution of $HgCl_2$ (825 mg, 3 mmol in 15 mL anhydrous methanol) was added dropwise with constant stirring to the solution of PMP (523 mg, 3 mmol in 10 mL anhydrous methanol) at room temperature. The resulting mixture was stirred under reflux at 60 °C for 3 h. After cooling, no precipitate was found. On evaporation of the solution in steam bath, yellow precipitate was obtained and dissolved in the mixture of ethanol (10 mL), chloroform (5 mL), and DMF (5 mL). After 3 d, light yellow crystals suitable for X-ray analysis were obtained,

washed with small amounts of ethanol and dried in a vacuum (Scheme 1). Yield: 77.3 %. Mp.: 240–241 °C (dec.). Elem. analysis for $C_{23}H_{23}Cl_4Hg_4N_5O_3$: calcd. C 20.29; H 1.70; N 5.14 %; found: C 20.26; H 1.73; N 5.18 %. **IR** (KBr): $\tilde{\nu}$ = 3435 w, 2935 m, 2858 m, 1715 m, 1614 s, 1593 s, 1498 s, 1456 w, 1363 m, 1319 m, 1294 s, 1195 w, 1117 w, 1073 w, 1003 w, 758 m, 692 m, 633m, 591 w, 504 w, 451 w cm^{-1}.

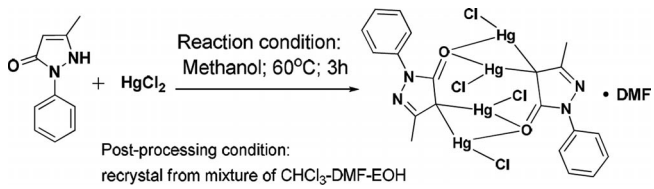

Scheme 1. Reaction scheme for the synthesis of **1**.

2.2 X-ray Crystallography

Diffraction data for a crystal of dimensions $0.21 \times 0.17 \times 0.16$ mm were collected with a BRUKER SMART CCD diffractometer with the graphite monochromated Mo-K_α (λ = 0.71073 Å) radiation by using the ω-2θ scan technique ($1.79 \leq \theta \leq 25.01°$) at 298(2) K. The crystal structure was solved by direct methods and Fourier synthesis (SHELXS-97),[24] and refined by full-matrix least-squares techniques on F^2 with the program SHELXL-97.[24] The carbon atoms (C11, C12, and C13) and the oxygen atom (O2) of DMF in **1** are both disordered over two positions, and all the site occupancy factors of C11, C12, C13, and O2 are 0.50. The non-hydrogen atoms, except C and O atoms in DMF, were refined anisotropically; and H atoms were added according to theoretical models. A summary of crystallographic data and refinement parameters is given in Table 1.

Table 1. Crystal data and structure refinement details for **1**.

Expirical formula	$C_{23}H_{23}Cl_4Hg_4N_5O_3$
Formula weight	1361.62
Color	Light yellow
Temperature /K	298(2)
Wavelength /Å	0.71073
Crystal system	triclinic
Space group	$P\bar{1}$
a /Å	7.4298(6)
b /Å	9.0313(8)
c /Å	12.4145(13)
α /°	108.949(2)
β /°	103.223(2)
γ /°	92.5950(10)
Volume /Å^3	760.50(12)
Z	1
$D_{calcd.}$ /Mg·m^{-3}	2.973
Absorption coefficient /mm^{-1}	20.511
F(000)	608
θ Range for data collection /°	1.79–25.01
Limiting indices	$-8 \leq h \leq 6$
	$-9 \leq k \leq 10$
	$-14 \leq l \leq 14$
Reflections collected	4010
Reflections independent, R(int)	2021, 0.0509
Goodness-of-fit on F^2	1.012
Final R indices [$I > 2\sigma(I)$]	0.0578, 0.1499
R indices (all data)	0.0733, 0.1632
Largest diff. peak and hole /e·Å^{-3}	3.312, –1.907

Crystallographic data (excluding structure factors) for the structure in this paper have been deposited with the Cambridge Crystallographic Data Centre, CCDC, 12 Union Road, Cambridge CB21EZ, UK. Copies of the data can be obtained free of charge on quoting the depository number CCDC-749487 (Fax: +44-1223-336-033; E-Mail: deposit@ccdc.cam.ac.uk, http://www.ccdc.cam.ac.uk).

2.3 Antibacterial Activity Determination

Compound **1** was evaluated for antibacterial activity against *coli bacillus*, *staphylococcus aureus*, and *bacillus subtilis* by the modified agar diffusion method.[25,26] The antibacterial activities of PMP and $HgCl_2$ were also tested for comparison. The compounds were dissolved in DMF. Nutrient agar thawed by heating in a water bath was transferred to plates and frozen at 37 °C. After the test strains were spread on the solid nutrient agar surface, stainless steel tubes (7.8 mm × 6 mm × 10 mm) were spread vertically on the surface. Samples (0.05 mL) with known concentration were injected into the steel tubes and allowed to incubate at 37 °C for 24 h. Inhibition zone around the disc was calculated as a zone diameter in millimeter. Blank tests showed that DMF used in the preparation of the sample solutions does not affect the test organisms.

2.4 DNA Binding Studies

Calf thymus DNA (CT-DNA) was dissolved in 5 mM Tris-HCl buffer at pH 7.43. CT-DNA in the buffer gave a ratio of UV absorbance at 260 nm and 280 nm and A_{260}/A_{280} of 1.85:1, which indicates that the DNA was free from protein.[27–28] The concentration of DNA was measured by absorption spectroscopy using the molar absorption coefficient (6600 mol^{-1}·cm^{-1}) at 260 nm.[27–28] Stock solutions were stored at 4 °C and used after no more than 4 d. Absorption spectral titration was performed by keeping the concentration of CT-DNA constant, while varying the title compound concentration. An equal volume of the title compound was added to the CT-DNA solution and a reference solution was added to eliminate the absorbance of the title compound itself.

For viscosity measurements, flow time was determined with a manually operated timer. Each sample was measured three-times to calculate the average flow time. Relative viscosities for DNA in the presence and absence of the title compound were calculated from the equation, $\eta = (t - t_0) / t_0$, where t is the observed flow time of the DNA-containing solution and t_0 is that of Tris-HCl buffer. Data were presented as $(\eta / \eta_0)^{1/3}$ vs. binding ratio, where η is the viscosity of CT-DNA in the presence of the title compound and η_0 is the viscosity of CT-DNA alone.[28–29]

2.5 Reagents and Instrumentation

CT-DNA was purchased from the Sigma Corp. All other chemicals were of reagent grade and used as received without further purification. IR spectra were recorded with a Spectrum One BFT-IR spectrophotometer as KBr pellets from 4000–450 cm^{-1}. Thermal analyses were performed on a NETZSCH STA 409PC differential thermal analyzer. The absorption spectra were determined at room temperature with a Shimadzu Uv-2550 ultraviolet-visible spectrophotometer. Viscosity measurements were carried out with an Ubbelodhe viscometer thermostatted at 25 ± 1 °C in a constant temperature bath.

3 Results and Discussion

3.1 Description of the Crystal Structure of 1

Single-crystal X-ray structural analysis indicates that **1** contains four Hg^{2+}, four Cl^-, two PMP^{2-} and one disordered DMF.

Zeitschrift für anorganische und allgemeine Chemie ZAAC Journal of Inorganic and General Chemistry

The ORTEP view of **1** with atomic labeling scheme is shown in Figure 1. Selected bond lengths and angles are given in Table 2. In **1**, each C2 atom of the pyrazolone ring from one PMP is bonded to two mercury ions, and the two mercury ions are coordinated to O1 atom from another PMP, thus forming a rare organomercury(II) dimer, $[Hg_2(PMP)Cl_2]_2$ (Figure 1). Furthermore, the bond lengths [C2–Hg1, 2.095(15) Å and C2–Hg2, 2.091(15) Å] are in the range of C–Hg covalent bond,[3,5,19,20,22] indicating the carbon and mercury atoms are bonded covalently in **1**. To the best of our knowledge, this is the first crystallographically characterized organomercury compound derived from PMP, and no study on two Hg^{II} attached to one carbon atom has been reported.[3,5,19,20,22] Furthermore, the mercury–mercury separation is 3.2735(8) Å, which is much shorter than the van der Waals distance for two mercury atoms (4.1 Å) and longer than the Hg–Hg single bond length (2.64 Å),[5,20,21] confirming the presence of a weak Hg···Hg interaction.

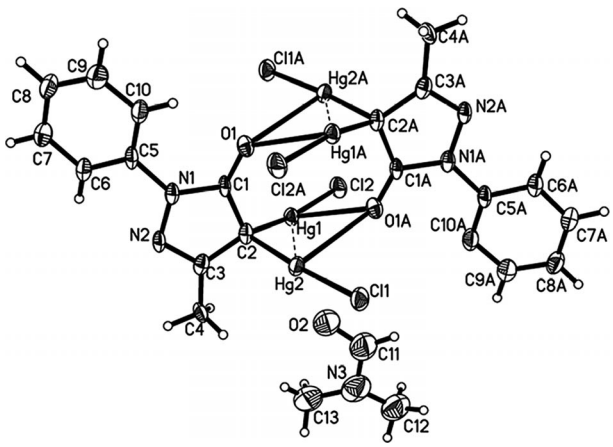

Figure 1. ORTEP view of **1** with the atom labeling scheme. The ellipsoids enclose 50% of the electronic density. Symmetry operator for equivalent position: A = –*x*+2, –*y*+1, –*z*+2.

Table 2. Selected bond lengths /Å and bond angles /° for **1**.

Bond lengths			
Hg(1)–C(2)	2.095(15)	O(2)–C(11)	1.23(8)
Hg(1)–Cl(2)	2.064(4)	O(2)–C(12)#1	1.31(9)
Hg(1)–Hg(2)	3.2735(8)	N(2)–C(3)	1.32(2)
Hg(2)–C(2)	2.091(15)	N(3)–C(11)	1.36(9)
Hg(2)–Cl(1)	2.310(4)	N(3)–C(11)#1	1.36(9)
Hg(1)–O(2)	3.13(4)	C(1)–C(2)	1.46(2)
Hg(2)–O(2)	3.05(4)	N(1)–N(2)	1.41(2)
O(1)–C(1)	1.23(2)		
Bond angles			
C(2)–Hg(1)–Cl(2)	170.0(5)	C(2)–Hg(1)–O(2)	80.4(9)
Cl(2)–Hg(1)–O(2)	107.2(8)	C(2)–Hg(2)–Cl(1)	176.1(5)
C(2)–Hg(2)–O(2)	82.5(9)	Cl(1)–Hg(2)–O(2)	98.9(8)
Cl(1)–Hg(2)–Hg(1)	139.44(12)	O(2)–Hg(2)–Hg(1)	59.2(7)

Symmetry transformations used to generate equivalent atoms: #1: –*x* + 2, –*y* + 1, –*z* + 2.

In the structure of **1**, each Hg^{II} is three-coordinate to one carbon atom from one PMP, one oxygen atom from another PMP and one terminal chlorine atom. The Hg–Cl bond lengths [Hg1–Cl2 2.306(4) Å and Hg2–Cl1 2.310(4) Å] are in the range of previously reported values [2.037(16)–2.816(3) Å].[5,19,30] The Hg–O bond lengths [Hg1–O1^A 2.7932(1) and Hg2–O1^A 2.9095(1) Å, *A*: –*x*+2,–*y*+1, –*z*+2] are longer than the reported usual lengths, but much shorter than the sum of the van der Waals radii (3.5 Å),[5,19,31] suggesting that the coordination interaction between mercury and oxygen atom is relatively weak. The local coordination arrangement of Hg^{II} is T-shaped with bond angles of 170.0(5)° for C2–Hg1–Cl2 and 176.1(5)° for C2–Hg2–Cl1. The slight deviation of the above-mentioned C–Hg–Cl bond angles from the linearity may be due to the coordination interaction of oxygen with Hg^{II}. Furthermore, two Hg–O bonds and two Hg–C bonds can form a quadrilateral (for instance C2–Hg1–O2^A–Hg2), in which the dihedral angle between C–Hg–Hg and O–Hg–Hg is 31.72(114)°. Two such quadrilaterals are connected by the C1 and C1^A atoms of pyrazole rings from two different PMP molecules, consequently constructing a unique polynuclear structure (Figure 1). As for the pyrazole ring, the coplanarity is not perfect (mean deviation from planarity is 0.0214 Å), and the dihedral angle between the pyrazole ring composed of C1C2C3N1N2 and the triangle of C2Hg1Hg2 is 87.61(49)°, nearly 90°; i.e. the two planes are almost perpendicular to each other.

On the other hand, the bond lengths of C1–O1 and C11–O2 are 1.23(2) and 1.23(8) Å, close to the typical C=O double bond of 1.210 Å.[32] The C3–N2 bond length [1.32(2) Å] belongs to C=N double bond (1.329 Å) in pyrazole,[32] whereas the C11–N3 distance [1.36(9) Å] falls into the range of conjugated C=N bond length (1.34–1.38 Å). The above-mentioned analyses of bond lengths indicate that the pyrazolone ring of PMP is present in the keto form.

In **1**, each ligand PMP bears two negative charges, because the C2 atom forms two covalent bonds with C1 and C3. And each C2 links to two Hg^{2+} ions, which are coordinated to one Cl^-, respectively. Consequently, the whole molecule is electroneutral.

Secondary bonds play an important role in the construction of mercury complexes or organomercury compounds.[19] Compound **1** exhibits three types of weak secondary interactions between the Hg^{II} and O atoms of DMF [intermolecular Hg1/Hg2···O2 interactions; contact distance of 3.128(4)/3.048(4) Å] or N of PMP [intermolecular Hg2···N2C interaction; contact distance of 3.115(2) Å, C: *x*, 1+*y*, *z*] or Cl [intermolecular Hg1D···Cl2/Cl1A interactions; contact distance of 3.307(4) / 3.314(4) Å, D: –1+*x*, *y*, *z* and A: 1–*x*, –*y*, 1–*z*, and intermolecular Hg2···Cl2A interactions; contact distance of 3.754(5) Å]. The above-mentioned Hg···O/N/Cl distances are close to the sum of the van der Waals radii of mercury (1.73–2.05 Å) and oxygen (1.52 Å) or nitrogen (1.55 Å) or chlorine (1.8 Å),[5,19,30] indicating that these secondary interactions in **1** are weak. Furthermore, there are two types of intermolecular C–H···Cl hydrogen bonds in **1**. Two hydrogen atoms of one methyl group of PMP from one organomercury dimer are hydrogen-bonded to two chlorine atoms from two other organomercury dimers; and one hydrogen atom of phenyl ring from the same PMP is hydrogen-bonded to the Cl1#1 atom from the

dimer, in which Cl#1 and Cl#3 coexist. Detailed data for the hydrogen bonds are given in Table 3. All the above-mentioned weak secondary Hg···N/O/Cl interactions and the intermolecular hydrogen bonds at the supramolecular level lead to a three-dimensional network (Figure 2). The hydrogen bonds and the Hg···N/O/Cl interactions in **1** are shown in Figure 3.

Table 3. Hydrogen bonding data /Å,° for **1**.

D–H···A	*d*(D–H)	*d*(H···A)	*d*(D···A)	(DHA)
C(6)–H(6)···Cl(1)#1	0.93	2.80	3.62(2)	147.6
C(4)–H(4A···Cl(2)#2	0.96	2.87	3.693(17)	144.9
C(4)–H(4C)···Cl(1)#3	0.96	2.83	3.744(18)	158.8

Symmetry transformations used to generate equivalent atoms: #1: $-x + 2, -y + 1, -z + 1$; #2: $x, y + 1, z$; #3: $x-1, y, z$;

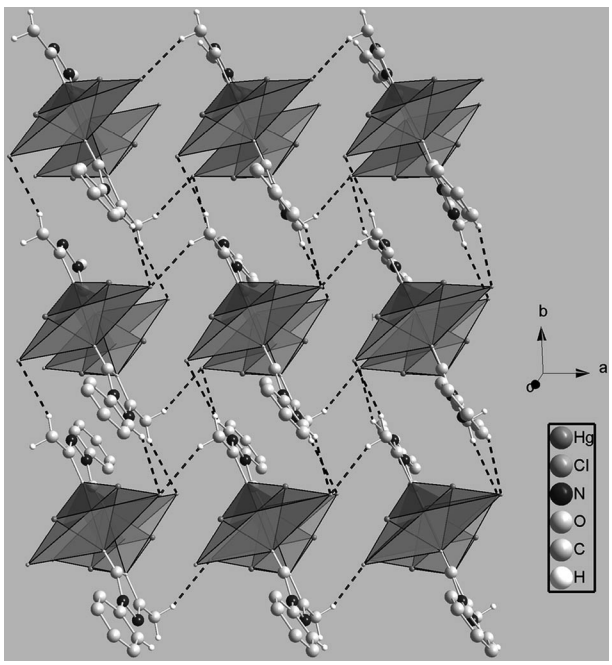

Figure 2. Ball and polyhedral representation of the packing diagram of **1** viewed along the *z* axis. The DMF molecules and hydrogen atoms not involved in the hydrogen bonds are omitted for clarity.

3.2 IR Spectroscopy

On comparing the infrared spectrum of the free PMP ligand, it is found that the strong band at 1599 cm^{-1} in PMP is split into two strong bands at 1614 cm^{-1} and 1593 cm^{-1} in **1**, which may be caused by the coordination of the carbonyl group to the mercury atom. Consequently, the band at 1614 cm^{-1} is assigned to the ν(C=O) vibration of the pyrazolone ring and the strong bands at 1593 cm^{-1} and 1498 cm^{-1} to the ν(C=C) vibration of the phenyl ring skeleton.[11,15,33] The absorption band at 633 cm^{-1} is the characteristic IV peak of amide caused by the bending vibration of O=C–N.[34] Furthermore, the broad medium band at 1715 cm^{-1} is ascribed to the tertiary amide ν(C=O) vibration of DMF.[34] The above assignments are in accordance with the crystal structure of **1**.

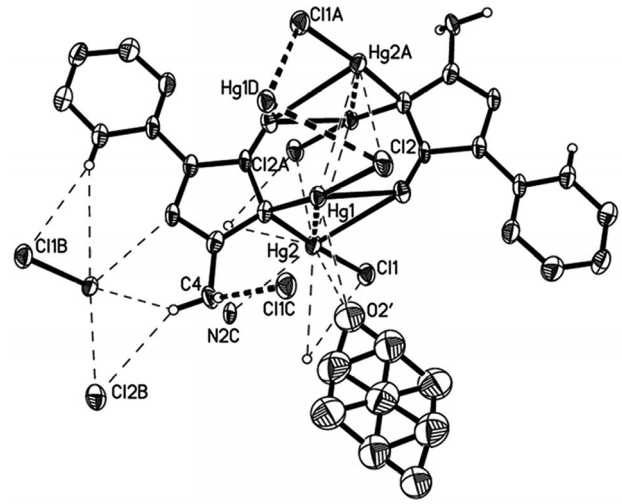

Figure 3. Intermolecular hydrogen bonds and the weak secondary Hg···N/O/Cl interactions of **1**. The hydrogen atoms not involved in hydrogen bonds are omitted for clarity.

3.3 Thermal Investigations

The thermal stability of **1** powder was studied by thermogravimetric (TG) analysis from 25–900 °C. The TG curve (Figure 4) showed two continuous weight loss steps during heating. **1** is stable up to 149 °C, at which point it begins to decompose. The weight loss of the first step in the range of 149–292 °C is 67.58 %, attributed to lose two $HgCl_2$ and two ligands PMP absence of carbonyl oxygen atoms (calcd. 66.49 %). In addition, the TG curves often clearly show individual steps of weight loss resulted from loss of absorbed or coordinated solvent molecules under 200 °C. In this case, such a step can't be found, indicating there is no DMF in **1** powder. Upon further heating, the second weight loss occurs and almost no residue remains over 659 °C.[35] The weight loss (31.03 %) at 292–900 °C can be assigned to loss of 2HgO (calcd. 33.51 %).

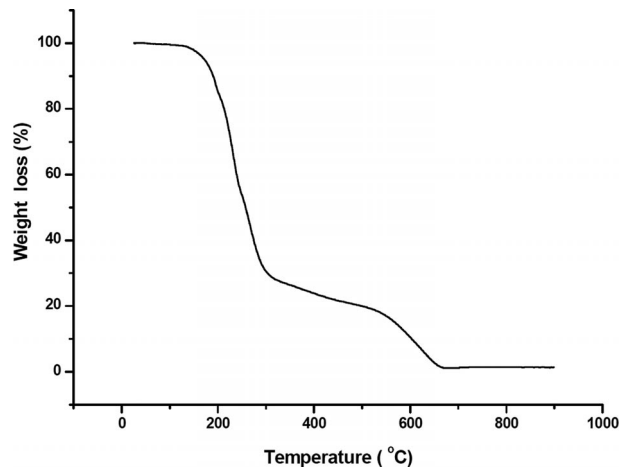

Figure 4. TG curve of **1**.

Zeitschrift für anorganische und allgemeine Chemie ZAAC Journal of Inorganic and General Chemistry

Table 4. Antibacterial activities of **1**, PMP, and mercury salt.

Compounds	Concentration /mg·mL^{-1}	Diameter of inhibition zone /mm		
		Escherichia coli	*Staphylococcus aureus*	*Bacillus subtilis*
$HgCl_2$	10	23.55	26.65	25.95
	5	17.35	23.85	24.25
	1	13.55	18.94	19.55
	0.1	9.10	10.85	10.50
PMP	10	15.21	16.13	15.35
	5	13.18	14.75	14.83
	1	11.43	13.32	11.57
	0.1	11.00	11.25	11.13
1	10	15.35	17.80	18.13
	5	14.10	17.65	17.58
	1	12.23	15.26	14.12
	0.1	11.68	11.71	13.51
DMF		7.82	7.82	7.81

3.4 Antibacterial Tests

The results (Table 4) show that **1**, free ligand PMP, and mercury chloride exhibit strong antibacterial activities against *Staphylococcus aureus*, *Bacillus subtilis*, and *Escherichia coli*, indicating the broad-spectrum properties of the compounds tested. Moreover, these compounds increase in activity with concentration for all the test strains.

Mercury chloride shows the highest activity against all the tested bacteria, when the concentration is greater than 0.1 mg·mL^{-1}, whereas **1** exhibits slightly higher activity than PMP. In general, compared to inorganic species, the corresponding organometallic compounds have a higher solubility in lipids, which makes it easier to diffuse through the lipidic matrix of the cellular membrane and hence increase the toxicity potential.[36,37] The fact that **1** with concentrations in the range of 1–10 mg·mL^{-1} exhibits lower antibacterial activity than the mercury salt may be a result of the high stability of **1**. It is difficult for **1** to release toxic mercury ions because of its high stability,[37–39] i.e. the existence of Hg–C covalent bonds, Hg–O coordinate bonds, and intermolecular Hg···N/Cl/O secondary interactions. In fact, the antibacterial activity of any compound is a complex combination of steric, electronic, and pharmacokinetic factors,[40] which makes it difficult to predict biological activity.

3.5 DNA Binding Experiments

3.5.1 Absorption Spectroscopy

The application of electronic absorption spectroscopy in DNA-binding studies is a useful technique.[41] The absorption spectra of CT-DNA in the presence and absence of **1** are given in Figure 5. Upon addition of increasing amounts of **1** to the solution of CT-DNA, a slight red shift (ca. 3 nm) and decrease in intensity of the absorption band (i.e. hypochromism is ca. 6.3 %) was observed, indicating weak binding of **1** to DNA. The changes of absorbance and wavelength may be ascribed to the intercalative binding with DNA. However, the decrease in the absorption intensity (hypochromism) is very much less than that observed for an intercalator like ethidium bromide.[42] Therefore, classical intercalation is ruled out for **1**. Because **1** is neutral, the electrostatic interaction between **1** and CT-DNA is also ruled out. Consequently, it is suggested that **1**, the organomercury dimer, binds to DNA in a groove-binding mode.

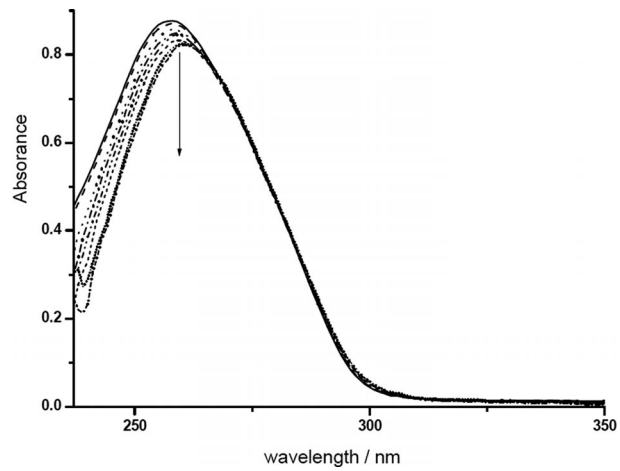

Figure 5. Absorption spectra of CT-DNA in the absence and presence of **1**. [DNA] = 132 μmol·L^{-1}, [1] = 0–140 μmol·L^{-1} from the top to bottom. The arrow indicates the change in absorbance upon increasing amounts of **1**.

3.5.2 Viscosity Measurements

To further explore the binding mode of **1** to CT-DNA, viscosity measurements were carried out. Under appropriate conditions, intercalation causes a significant increase in the viscosity of DNA solutions due to an increase in the separation of the base pairs at the intercalation sites. An increase in the overall DNA contour length can be observed.[43] In contrast, compounds that bind exclusively in DNA grooves, under the same conditions, typically cause less pronounced change (positive or negative) or no change in DNA solution viscosity.[43] The effect of **1** on the viscosity of DNA is depicted in Figure 6. With increasing amounts of **1**, the relative viscosity of DNA increases very slowly. In other words, the addition of **1** to CT-DNA does not lead to significant change in relative specific viscosity, which indicates that **1** binds CT-DNA by groove

binding mode instead of intercalation. This result is consistent with the above-mentioned absorption spectral experimental result.

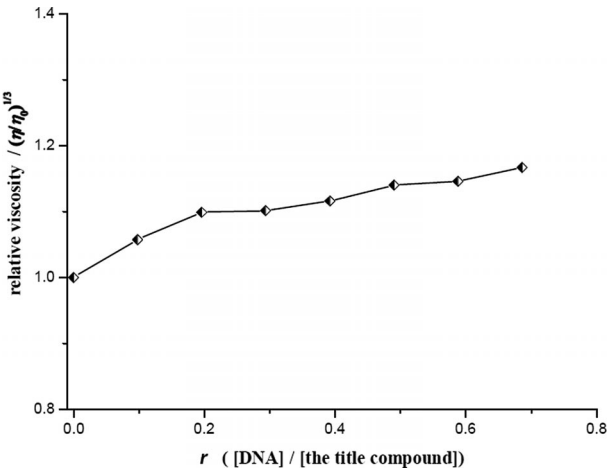

Figure 6. Effect of increasing amounts of **1** on the relative viscosity of CT-DNA at 25 ± 1 °C.

4 Conclusions

The organomercury dimer $[Hg_2(PMP)Cl_2]_2$·DMF (**1**) was synthesized and characterized by elemental analysis, IR spectroscopy, TG, and single-crystal X-ray diffraction analysis. The DNA binding properties of **1** were investigated by absorption spectroscopy and viscosity measurements. Experimental results indicate that **1** can bind to DNA by groove binding mode. In addition, antibacterial tests showed that **1** features strong and broad-spectrum antibacterial activities against tested bacteria.

Acknowledgements

This work is supported by Jiangsu Postdoctoral Science Foundation (1201049C), the Science and Technique Foundation of Lianyungang (CG1132), the College Students Practice and Innovation Training Project of Jiangsu Province, and the Project funded by the Priority Academic Program Development of Jiangsu Higher Education Institutions.

References

[1] A. M. Asaduzzaman, G. Schreckenbach, *Inorg. Chem.* **2011**, *50*, 3791.
[2] C. K. Prudenté, M. C. Hausman, *Bioconjugate Chem.* **2003**, *14*, 1270.
[3] Y. Liu, P. F. Yan, Y. H. Yu, G. F. Hou, J. S. Gao, *Inorg. Chem. Commun.* **2010**, *13*, 630.
[4] P. V. Solntsev, W. R. Goetsch, V. N. Nemykin, *Organometallics* **2011**, *30*, 6636.
[5] R. S. Baligar, S. Sharma, H. B. Singh, R. J. Butcher, *J. Organomet. Chem.* **2011**, *696*, 3015.
[6] V. Chandrasekhar, A. Kumar, M. D. Pandey, *J. Organomet. Chem.* **2010**, *695*, 74.
[7] J. M. Bramlett, H. J. Im, X. H. Yu, T. N. Chen, H. Cai, L. E. Roecker, C. E. Barnes, S. Dai, Z. L. Xue, *Inorg. Chim. Acta* **2004**, *357*, 243.
[8] X. Y. Tang, A. X. Zheng, H. Shang, R. X. Yuan, H. X. Li, Z. G. Ren, J. P. Lang, *Inorg. Chem.* **2011**, *50*, 503.
[9] M. Kim, T. J. Taylor, F. P. Gabbai, *J. Am. Chem. Soc.* **2008**, *130*, 6332.
[10] Z. G. Yang, Z. Wang, S. Bzi, X. H. Liu, L. L. Lin, X. M. Feng, *Org. Lett.* **2011**, *13*, 596.
[11] V. M. Leovac, G. A. Bogdanović, L. S. Jovanović, L. Joksović, V. Marković, M. D. Joksović, S. M. Denčić, A. Isaković, I. Marković, F. W. Heinemann, S. Trifunović, I. Dalović, *J. Inorg. Biochem.* **2011**, *105*, 1413.
[12] G. Cerchiaro, A. M. D. C. Ferreira, A. B. Teixeira, H. M. Magalhes, A. C. Cunha, V. F. Ferreira, L. S. Santos, M. N. Eerlin, J. M. S. Skakle, S. M. S. V. Wardell, J. L. Wardell, *Polyhedron* **2006**, *25*, 2055.
[13] S. Abe, K. Kirima, K. Tsuchiya, M. Okamoto, T. Hasegawa, H. Houchi, M. Yoshizumi, T. Tamaki, *Chem. Pharm. Bull.* **2004**, *52*, 186.
[14] X. Qi, Y. Okuma, T. Hosoi, Y. Nombra, *J. Pharmacol. Exp. Therap.* **2004**, *311*, 388.
[15] R. B. Xu, X. Y. Xu, Y. H. Yin, M. Y. Wang, X. J. Yang, Q. Q. Xu, L. P. Ma, *J. Coord. Chem.* **2009**, *62*, 3905.
[16] R. B. Xu, X. Y. Xu, S. A. Li, X. J. Yang, D. Q. Wang, Y. P. Huang, C. M. Xu, *Struct. Chem.* **2010**, *21*, 1085.
[17] R. B. Xu, Y. Y. Li, M. Tian, M. Y. Wang, D. Q. Wang, W. X. Ma, X. J. Yang, X. Y. Xu, *J. Inorg. Organomet. Polym. Mater.* **2012**, *22*, 1062.
[18] M. Wilhelm, S. Deeken, E. Berssen, W. Saak, A. Lützen, R. Koch, H. Strasdeit, *Eur. J. Inorg. Chem.* **2004**, *11*, 2301.
[19] J. S. Casas, M. S. García-Tasende, J. Sordo, *Coord. Chem. Rev.* **1999**, *193*, 283.
[20] Z. L. Zhu, M. Brynda, R. J. Wright, R. C. Fischer, W. A. Merrill, E. Rivard, R. Wolf, F. C. Fettinger, *J. Am. Chem. Soc.* **2007**, *129*, 10847.
[21] M. R. Haneline, M. Tsunoda, F. P. Gabbai, *J. Am. Chem. Soc.* **2002**, *124*, 3737.
[22] U. Patel, S. Sharma, H. B. Singh, S. Dey, W. K. Jain, G. Wolmershäuser, R. J. Butcher, *Organometallics* **2010**, *29*, 4265.
[23] B. Soro, S. Stoccoro, G. Minghetti, A. Zucca, M. A. Cinellu, S. Gladiali, M. Manassero, M. Sansoni, *Organometallics* **2005**, *24*, 53.
[24] G. M. Sheldrick, *Acta Crystallogr., Sect. A* **2008**, *64*, 112.
[25] J. Gao, X. Y. Xu, W. X. Ma, M. Y. Wang, H. B. Song, X. J. Yang, L. L. De, X. Wang, *J. Coord. Chem.* **2004**, *57*, 1553.
[26] T. T. Xu, J. Gao, X. Y. Xu, D. Q. Wang, *Chin. J. Inorg. Chem.* **2008**, *24*, 1582.
[27] N. M. Aghatabay, A. Neshat, T. Karabiyik, M. Somer, D. Haciu, B. Dülger, *Eur. J. Med. Chem.* **2007**, *42*, 205.
[28] N. Raman, A. Sakthivel, R. Jeyamurugan, *J. Coord. Chem.* **2010**, *63*, 1080.
[29] H. H. Liu, Y. T. Li, Z. Y. Wu, K. Zheng, C. W. Yan, *J. Coord. Chem.* **2011**, *64*, 1360.
[30] S. Park, S. Y. Lee, S. S. Lee, *Inorg. Chem.* **2010**, *49*, 1238.
[31] G. B. Deacon, P. W. Felder, P. C. Junk, K. Müller-Buschbaum, T. J. Ness, C. C. Quitmann, *Inorg. Chim. Acta* **2005**, *358*, 4389.
[32] F. Marchetti, C. Pettinari, R. Pettinari, A. Cerquetella, A. Cingolani, E. J. Chan, K. Kozawa, B. W. Skelton, A. H. White, R. Wanke, M. L. Kuznetsov, L. M. D. R. S. Marins, A. J. L. Pombeiro, *Inorg. Chem.* **2007**, *46*, 8245.
[33] G. A. Chmutova, O. N. Kataeva, H. Ahlbrecht, A. R. Kurbangalieva, A. I. Movchan, A. T. H. Lenstra, H. J. Geise, A. T. H. Lenstra, *J. Mol. Struct.* **2001**, *570*, 215.
[34] Q. F. Deng, L. Liu, H. M. Deng, *Spectrum Analysis Course*, Beijing, Science Press, **2003**.
[35] G. Mahmoudi, A. Morsali, *Cryst. Growth Des.* **2008**, *8*, 391.
[36] M. E. Crespo-López, G. L. Macêdo, S. L. D. Pereira, G. P. F. Arrifano, D. L. W. Picanço-Diniz, J. L. M. do Nascimento, A. M. Herculano, *Pharm. Res.* **2009**, *26,* 212.
[37] M. N. Patel, P. A. Dosi, B. S. Bhatt, *Spectrochim. Acta Part A* **2012**, *86*, 508.

[38] T. G. Roy, S. K. S. Hazari, B. K. Dey, H. A. Meah, M. S. Rahman, D. I. Kim, Y. C. Park, *J. Coord. Chem.* **2007**, *60*, 1567.
[39] S. W. Bi, S. X. Liu, *Chin. J. Inorg. Chem.* **1996**, *12*, 423.
[40] K. N. Thimmaiah, G. T. Chandrappa, W. D. Lloyd, C. Párkányi, *Transition Met. Chem.* **1985**, *10*, 299.
[41] X. C. Yang, Y. N. Liu, S. T. Yao, Y. Xia, Q. Li, W. J. Zhang, L. M. Chen, J. Liu, *J. Coord. Chem.* **2011**, *64*, 1491.
[42] S. Satyanarayana, J. C. Dabrowiak, J. B. Chaires, *Biochemistry* **1993**, *32*, 2573.
[43] J. M. Veal, R. L. Rill, *Biochemistry* **1991**, *30*, 1132.

Received: April 17, 2013
Published Online: July 2, 2013

